AD 294 472

ARPA ORDER NO. 347-62
PROJECT CODE NO. 7400

GENERAL MOTORS CORPORATION

TECHNICAL REPORT
ON

PLASMA FREQUENCY AND ELECTRON COLLISION FREQUENCY CHARTS FOR HYPERSONIC VEHICLE EQUILIBRIUM FLOW FIELDS IN AIR

CONTRACT NUMBER DA-04-495-ORD-3567
HYPERVELOCITY RANGE RESEARCH PROGRAM

DEFENSE RESEARCH LABORATORIES
SANTA BARBARA, CALIFORNIA

AEROSPACE OPERATIONS DEPARTMENT

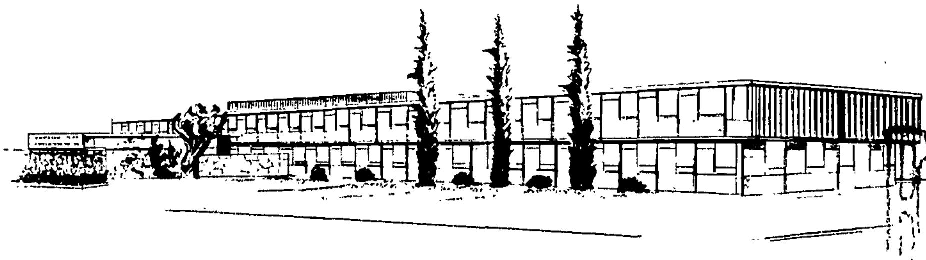

TR62-209C

DECEMBER 1962

ARPA ORDER NO. 347-62
PROJECT CODE NO. 7400

Copy No 25

GENERAL MOTORS CORPORATION

TECHNICAL REPORT
ON

PLASMA FREQUENCY AND ELECTRON COLLISION FREQUENCY CHARTS FOR HYPERSONIC VEHICLE EQUILIBRIUM FLOW FIELDS IN AIR

PREPARED BY HENRY M. MUSAL, JR.

CONTRACT NUMBER DA-04-495-ORD-3567
HYPERVELOCITY RANGE RESEARCH PROGRAM

DEFENSE RESEARCH LABORATORIES
SANTA BARBARA, CALIFORNIA

AEROSPACE OPERATIONS DEPARTMENT

TR62-209C

DECEMBER 1962

ABSTRACT

The purpose of this report is to present charts of plasma frequency and electron collision frequency as functions of air density (altitude) and vehicle velocity for selected regions of equilibrium hypersonic flow fields, with a brief description of the method of derivation and the area of applicability.

The two particular regions of the flow field treated here are the stagnation region and the end-point of the isentropic (expansion controlled) part of the wake of a blunt body. The charts cover the altitude range from zero to 350, 000 feet and the velocity range from 6, 000 to 40, 000 feet/second. *

* This research is a part of Project DEFENDER, Sponsored by The Advanced Research Projects Agency, Department of Defense.

INTRODUCTION

At the present time, some of the properties of hypersonic vehicle flow fields in air can be theoretically predicted under certain assumptions and in particular parameter regimes. The two basic properties of greatest importance to the study of electromagnetic wave propagation in these flow fields are the plasma frequency and the electron collision frequency. Preliminary charts of these properties as functions of the aerodynamic variables have been prepared for selected parts of the flow field of a hypersonic blunt body. The regions of the flow field treated here are the stagnation region and the end-point of the isentropic (expansion controlled) part of the wake.

Using air density (altitude) and vehicle velocity as the aerodynamic variables, the maps cover the range from zero to 350, 000 feet and from 6, 000 to 40, 000 feet/second, respectively. A brief description of these charts, the theoretical background upon which they are based, and the regime of applicability follow.

The charts presented here for the plasma frequency and electron collision frequency in hypersonic flow fields were derived on the basis of a number of assumptions that are not always met in aerodynamic situations of interest. That is, when the body is not blunt,

when chemical equilibrium is not maintained throughout the flow field, or when the flow is turbulent, the actual values of these quantities can be expected to depart significantly from the values given here. The purpose of these charts is more to indicate general trends rather than to represent exact results. However, the calculations have been carefully made so that when the assumptions are met the results should be accurate.

Symbols

f_p = plasma frequency (cycles/sec)
N_e = electron concentration (electrons/meter^3)
ν_c = electron collision frequency (collisions/sec)

CHART DERIVATION

STAGNATION REGION

The plasma frequency and electron collision frequency for air behind a normal shock (the stagnation region of the blunt body flow field) are shown as functions of ambient density (altitude) and shock velocity in Figure 1. The basic assumption involved here is that the air is in chemical equilibrium. The plasma frequency (f_p) was calculated from the electron concentration in the usual manner ($f_p = 8.977\sqrt{N_e}$), where the electron concentration (N_e) was taken from Hochstim's[1] chart of normal shock properties. The electron collision frequency (ν_c) was then obtained from Musal's [2] report for the temperature and density of the shocked air obtained from Hochstim's chart. Since the electron collision frequency for air at temperatures above 8, 000° K was not calculated in this report, the electron collision frequency contours in Figure 1 do not extend to the very high velocity regime where such temperatures are encountered. It is in this regime that the ion concentration becomes sufficiently large to become the dominant contributor to the electron collision frequency, at which point the concept of binary collisions between electrons and other particles (upon which the electron collision frequency calculation is based) becomes inadequate to handle the calculation correctly.

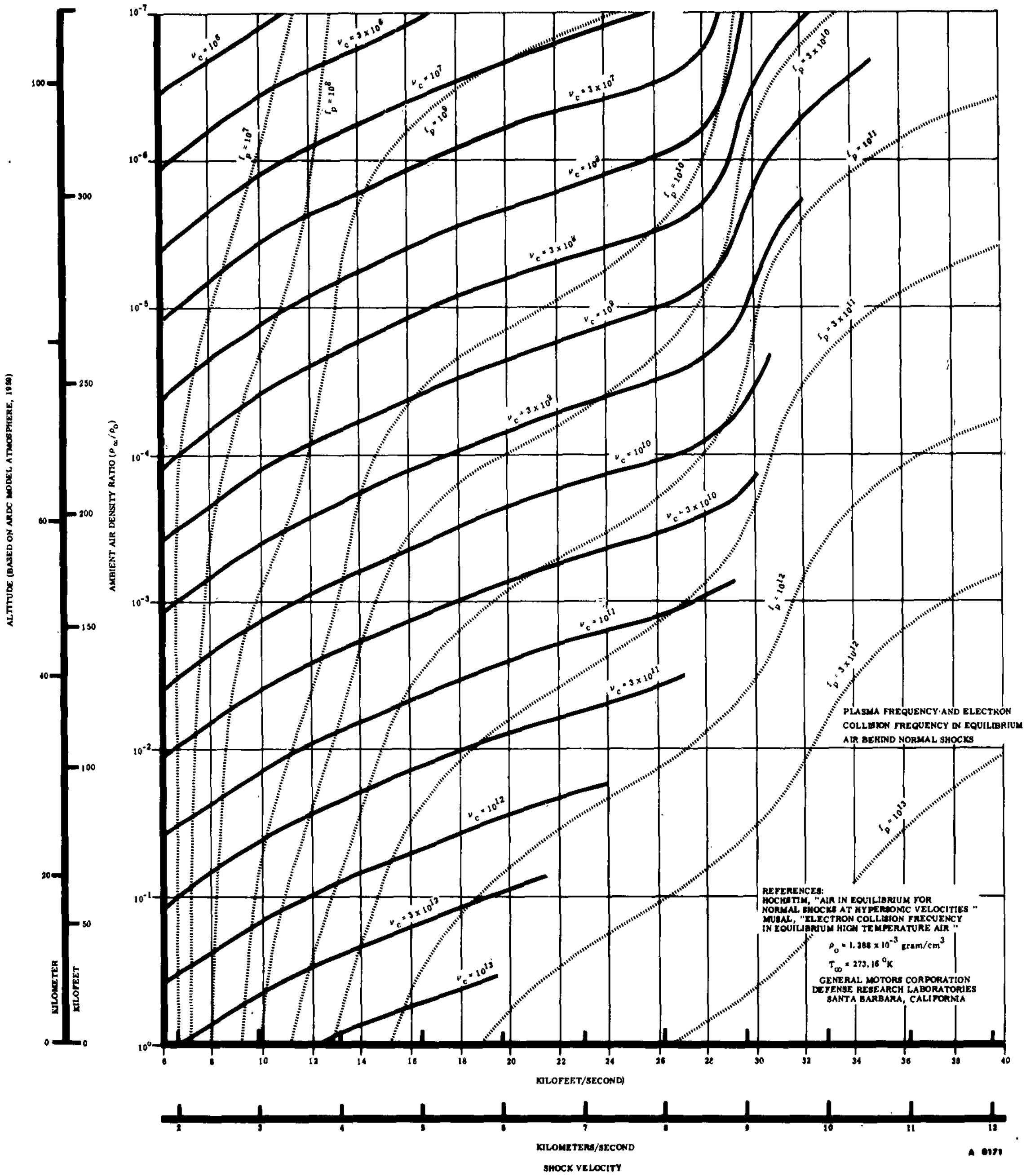

Figure 1 PLASMA FREQUENCY AND ELECTRON COLLISION FREQUENCY IN EQUILIBRIUM AIR BEHIND NORMAL SHOCKS

It may be seen from Figure 1 that the plasma frequency depends most strongly upon the shock velocity, although the ambient density also has a significant influence. The electron collision frequency depends most strongly on the ambient density except at very high velocities.

ISENTROPIC WAKE

The theoretical study of the flow field behind a hypersonic blunt body (the wake or trail) is extremely complex and still a subject of advanced research. Recently Feldman[3] has given an excellent description and analysis of certain aspects of this problem, which will not be repeated except for those points directly related to the results presented here. Following Feldman, the wake behind a hypersonic blunt body is considered to be composed of two regions, first the isentropic (expansion-controlled) wake immediately following the body and behind this the isobaric (conduction or diffusion-controlled) wake, or trail, as shown in Figure 2.

The isentropic wake is assumed to be formed from the hot compressed air in the stagnation region flowing around and behind the body in an equilibrium, laminar, isentropic expanding flow. This expansion stops when the pressure in the wake decreases to the ambient pressure, which marks the end-point of the isentropic wake and the starting point of the isobaric wake. The stream tube from the stagnation point at the front of the body becomes the axial stream tube in the wake when the flow closes behind the body, neglecting the effect of the viscous boundary layer gas which actually flows into the wake core and occupies the axial region of the wake. The air properties

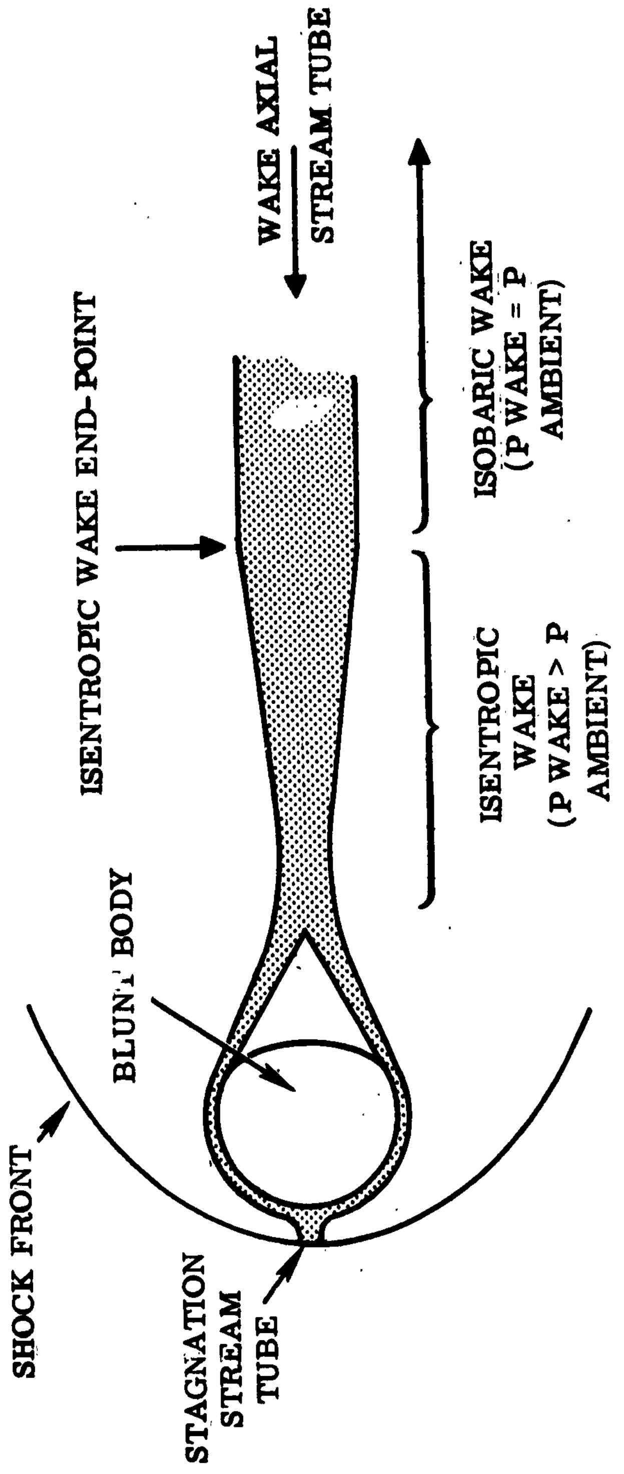

A 0172

Figure 2 Wake Nomenclature

are determined along this stream tube from the stagnation point conditions (given by the Hochstim chart) by an isentropic expansion to ambient pressure through the use of the Mollier diagram for equilibrium air [4]. The temperature and density thus determined at the isentropic wake end-point are used to find the electron concentration and electron collision frequency from Hochstim and Musal, respectively. The plasma frequency is then calculated as before.

Figure 3 shows the plasma frequency and electron collision frequency on the wake axis at the end-point of the isentropic wake as functions of the ambient density (altitude) and velocity of the body generating the wake. It should be pointed out that because these end-point properties are affected slightly by the ambient temperature, the chart is properly constructed in terms of ambient density and an ambient temperature equal to the reference temperature but not in terms of altitude because of the ambient temperature variation with altitude [5]. However, the temperature variations with altitude do not change the end-point values by more than a factor of two under the worst conditions. The direction of change is an increase in both the plasma frequency and the electron collision frequency with an increase in the ambient temperature. The fact that the entire ranges of ambient density and velocity are not covered in this chart is the result of an insufficient range of variables covered in the Mollier diagram. Although the distance behind the body at which the isentropic wake end-point occurs is of interest, it unfortunately cannot be obtained by the simple approach used here.

It may be seen from Figure 3 that the electron collision frequency depends almost solely on the ambient density. At low velocities the plasma frequency depends strongly on velocity; at high velocities

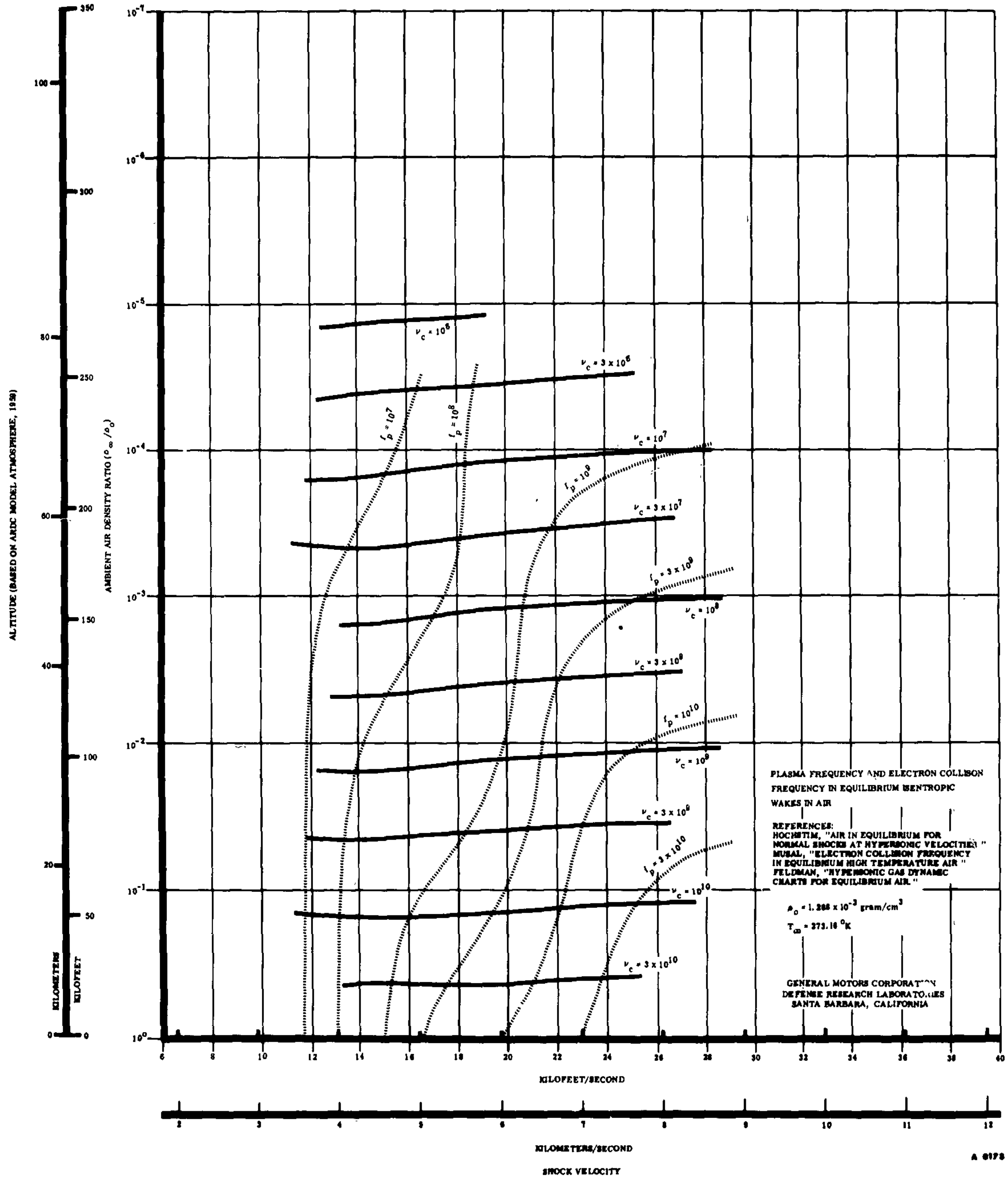

Figure 3 PLASMA FREQUENCY AND ELECTRON COLLISION FREQUENCY IN EQUILIBRIUM ISENTROPIC WAKES IN AIR

there is strong dependence on ambient density. That is, it can be seen that at increasingly high velocities the plasma frequency tends to remain relatively constant.

Some mention of the effects to be expected when the actual flow field conditions deviate from the assumed conditions should be made. Non-equilibrium conditions can affect the plasma frequency considerably, either increasing or decreasing it depending upon the region of the flow field in which the onset of non-equilibrium occurs. Onset of non-equilibrium behind the body would most likely cause the plasma frequency in the wake to remain at higher values than depicted in the chart. Non-equilibrium onset occurring in the stagnation region affects the plasma frequency in the wake in a generally unpredictable manner. Turbulence in the wake will tend to cool the central core, causing the plasma frequency to decrease below the values shown in the chart.

CONCLUDING REMARKS

Figure 4, composed from Figures 1 and 3, gives both the plasma frequency in the stagnation region and the isentropic wake end-point in order to show the large range of variation encountered in the flow field from the stagnation point to the isentropic wake end-point. It may be seen that the plasma frequency decreases two or three orders of magnitude from the stagnation point to the end-point of the isentropic wake.

In principle, the results presented here are contained in the original referenced works of Hochstim, Feldman and Musal. However,

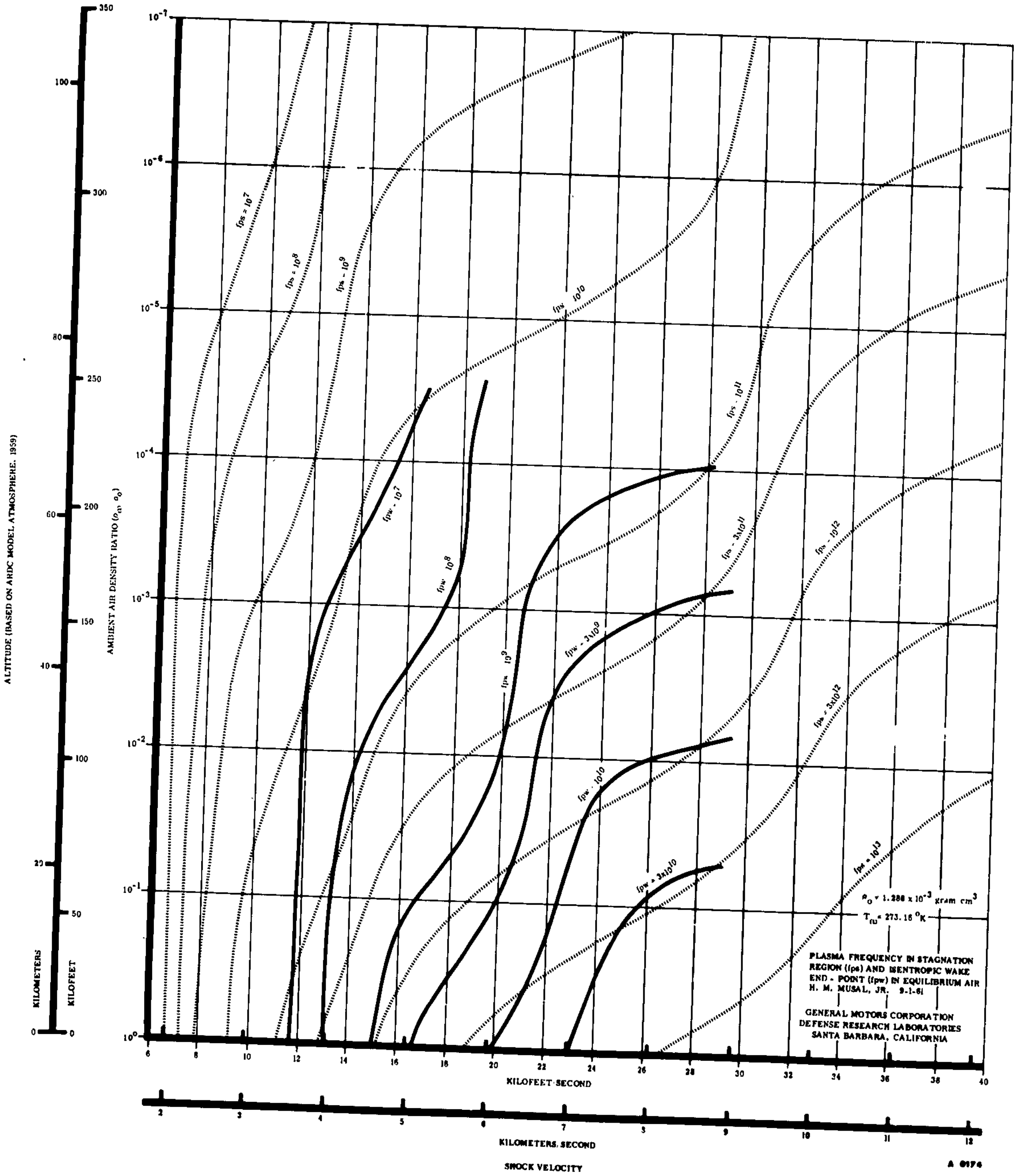

Figure 4 PLASMA FREQUENCY IN STAGNATION REGION (fps) AND ISENTROPIC WAKE END-POINT (fpw) IN EQUILIBRIUM IN AIR

neither Hochstim nor Feldman (in their primarily aerodynamic studies) give the electron collision frequency in the flow field, an essential parameter for electromagnetic considerations. Feldman (in the wake studies) has given complete and detailed results for a few specific cases, whereas the objective of this study is to cover a broad range of aerodynamic variables without the extensive computational effort required in the detailed analysis. Thus, the wake results presented here are not so comprehensive and detailed as could be obtained using Feldman's approach. However, the extensive range of variables covered here gives a broad survey of the electromagnetic properties of the flow field over a wide range of flight conditions.

REFERENCES

(1) General Dynamics, Convair Division, by A. R. Hochstim, Air in Equilibrium for Normal Shocks at Hypersonic Velocities Included with ZPh-(GP) - 002, San Diego, January 1958

(2) H. M. Musal, Jr., "Electron Collision Frequency in Equilibrium High Temperature Air", Research Note 9, 1 May 1960, Bendix Systems Division, Ann Arbor, Michigan

(3) S. Feldman, "On Trails of Axisymmetric Hypersonic Blunt Bodies Flying Through the Atmosphere", J. Aerospace Sci., Vol. 28, No. 6, June 1961, pp. 433-448

(4) S. Feldman, "Hypersonic Gas Dynamic Charts for Equilibrium Air", Research Report 40, January 1957, AVCO Research Laboratory, Everett, Massachusetts

(5) Air Research and Development Command, Air Force Cambridge Center, The ARDC Model Atmosphere, 1959, by R. A. Minzner, K. S. W. Champion, and H. L. Pond, AFCRC-TR-59-267, Bedford, Massachusetts, August 1959

DISTRIBUTION

Recipient	Copy No.
Commander, U.S. Army Missile Command Redstone Arsenal, Alabama ATTN: ORDXM-RRX	1-12
Advanced Research Projects Agency The Pentagon Washington 25, D.C. ATTN: Lt. Col. Cooper Ballistic Missile Defense Office	13, 14
Aerojet-General Corporation Azusa, California ATTN: C. Dunning	15
Aeronutronic Division Ford Motor Company 1234 Air Way Glendale, California ATTN: Dr. John Hall	16
Aerospace Corporation P.O. Box 4007 Patrick AFB, Florida ATTN: Dr. Martin Gould Classified Documents Control	17
Aerospace Corporation Classified Information Control 2400 E. El Segundo Blvd El Segundo, California ATTN: Dr. D. Bitondo	18
Aerospace Technical Intelligence Center U.S. Air Force Wright-Patterson Air Force Base, Ohio ATTN: AFCIN-4F3B	19
Air Force Ballistic Missile Division BSRUT AF Unit Post Office Los Angeles 45, California ATTN: Major William W. Levy	20
Air Force Command and Control Dev. Div. Air Research and Development Command L. G. Hanscom Field Bedford, Massachusetts ATTN: CCO-Range Measurements Office	21

Recipient	Copy No.
Headquarters ARDC Andrews Air Force Base Washington 25, D.C. ATTN: RDRC	22
Armed Services Tech. Infor. Agency Arlington Hall Station Arlington 12, Virginia ATTN: J. Heaton Heald	23-32
Research and Advanced Dev. Div. Avco Corporation Wilmington, Massachusetts ATTN: H.S. Flickinger Chief, Data Evaluation and Analysis	33
Avco-Everett Research Laboratory 2385 Revere Beach Parkway Everett, Massachusetts	34
Ballistics Research Laboratories Exterior Ballistics Laboratory Aberdeen, Maryland ATTN: Dr. C. Murphy	35
Barnes Engineering Company 30 Commerce Road Stamford, Connecticut	36
Batelle Memorial Institute 505 King Avenue Columbus 1, Ohio ATTN: Battelle-Defender	37
Bell Telephone Laboratories, Inc. Whippany, New Jersey ATTN: Mr. C.W. Hoover, Rm 2B-105	38
The Bendix Corporation Bendix Systems Division 3300 Plymouth Road Ann Arbor, Michigan ATTN: Systems Analysis and Mathematics Dept.	39
Commanding Officer Bureau of Naval Weapons Washington, D.C. ATTN: FASE, Dept. of the Navy	40

Recipient	Copy No.
Chief, Bureau of Naval Weapons Navy Department Washington 25, D. C. ATTN: RMWC-322	41
Brown Engineering Company Custodian, Central Security Files P.O. Drawer 917 Huntsville, Alabama ATTN: H. Crews	42
Cornell Aeronautical Laboratory, Inc. 4455 Genesee Street Buffalo 21, N. Y. ATTN: J. Lotsof W. Wurster	43, 44
Electro-Optical Systems, Inc. 125 N. Vinedo Avenue Pasadena, California ATTN: Mr. Denison	45
General Dynamics/Astronautics San Diego, California ATTN: Mr. K. G. Blair Chief Librarian Mail Zone 6-157 for W. Hooker 6-172	46
General Electric Company - MSVD Space Sciences Laboratory 3750 D Street Philadelphia, Pa. ATTN: Re-Entry Physics Library	47
Technical Information Center General Electric Company, MSVD Room 3446, 3198 Chestnut Street Philadelphia 4, Pa. ATTN: Mr. Lawrence I. Chasen Manager, Tech Info Center	48
Geophysics Corporation of America Burlington Road Bedford, Massachusetts ATTN: John W. Bond, Jr.	49
Heliodyne Corporation 2365 Westwood Blvd. Los Angeles, California	50
Jet Propulsion Laboratory 4800 Oak Grove Drive Pasadena, California ATTN: Hunston Denslow Library Supervisor	51

Recipient	Copy No.
Applied Physics Laboratory The John Hopkins University 8621 Georgia Avenue Silver Spring, Maryland ATTN: Mr. George L. Seielstad	52
Kaman Nuclear Division Colorado Springs, Colorado ATTN: Dr. A. P. Bridges	53
Instrument Research Division Langley Research Center Langley Field, Virginia ATTN: Howard B. Edwards	54
Lincoln Laboratory, MIT P. O. Box 73 Lexington 73, Massachusetts ATTN: Library, D-224 G. Pippert	55
Lockheed Missiles and Space Division Sunnyvale, California ATTN: Ray Munson	56
Melpar Inc. Applied Science Division 11 Galen Street Watertown 72, Massachusetts ATTN: M. J. Cryer	57
The MITRE Corporation Bedford, Massachusetts ATTN: Supervisor Library Services	58
Office of the Director Technical Analysis and Advisory Group (OP-07T3E) Deputy Chief of Naval Operations (Development) The Pentagon Washington 25, D. C.	59
Chief of Naval Operations Navy Department Washington 25, D. C. ATTN: OP732	60
Chief of Ordnance Hdqt. Dept. of the Army Washington 25, D. C. ATTN: ORDTU	61

Recipient	Copy No.
RAND Corporation 1700 Main Street Santa Monica, California ATTN: Library (M. H. Davis)	62
Raytheon Company Missile Systems Division Bedford Res. and Dev. Center Bedford, Massachusetts ATTN: Mrs. I. Britton, Librarian	63
Stanford Research Institute Documents Center Menlo Park, California ATTN: Acquisitions	64
Space Technology Laboratories P.O. Box 95001 Los Angeles 45, California ATTN: Mr. L. McFadden	65
Space Technology Laboratories Titan Program Director P.O. Box 95001 Los Angeles, California ATTN: A. C. Anchordough	66
Special Projects Office Department of the Navy Washington 25, D.C. ATTN: SP-2721	67
The Radiation Laboratory Department of Electrical Eng. University of Michigan 201 E. Catherine Ann Arbor, Michigan ATTN: Dr. Richard J. Leite	68
University of Michigan Willow Run Laboratories Technical Document Service P.O. Box 2008 Ann Arbor, Michigan ATTN: Bamirac Library/B. R. George	69
Command and Control Systems Division Directorate of Systems Development Headquarters, Room 4D324 The Pentagon Washington 25, D.C. ATTN: Major R. J. Kaminski U.S. Air Force	70

Recipient	Copy No.
Commanding General U.S. Army Air Defense Command Ent Air Force Base Colorado Springs, Colorado ATTN: Advanced Projects Division, G-3	71
Commander U.S. Army Ordnance Missile Command Redstone Arsenal, Alabama ATTN: Technical Library	72
U.S. Army Liaison Office Canadian Armament Res and Dev Establishment P.O. Box 1427 Quebec, P.Q., Canada ATTN: Lt. Col. E. W. Kreischer	73
Director U.S. Naval Research Laboratory Washington 25, D.C. ATTN: Code 2027	74
Director Weapons Systems Evaluation Group Pentagon, Room 1E800 Washington 25, D.C.	75
Defense Research Laboratories	76 and above

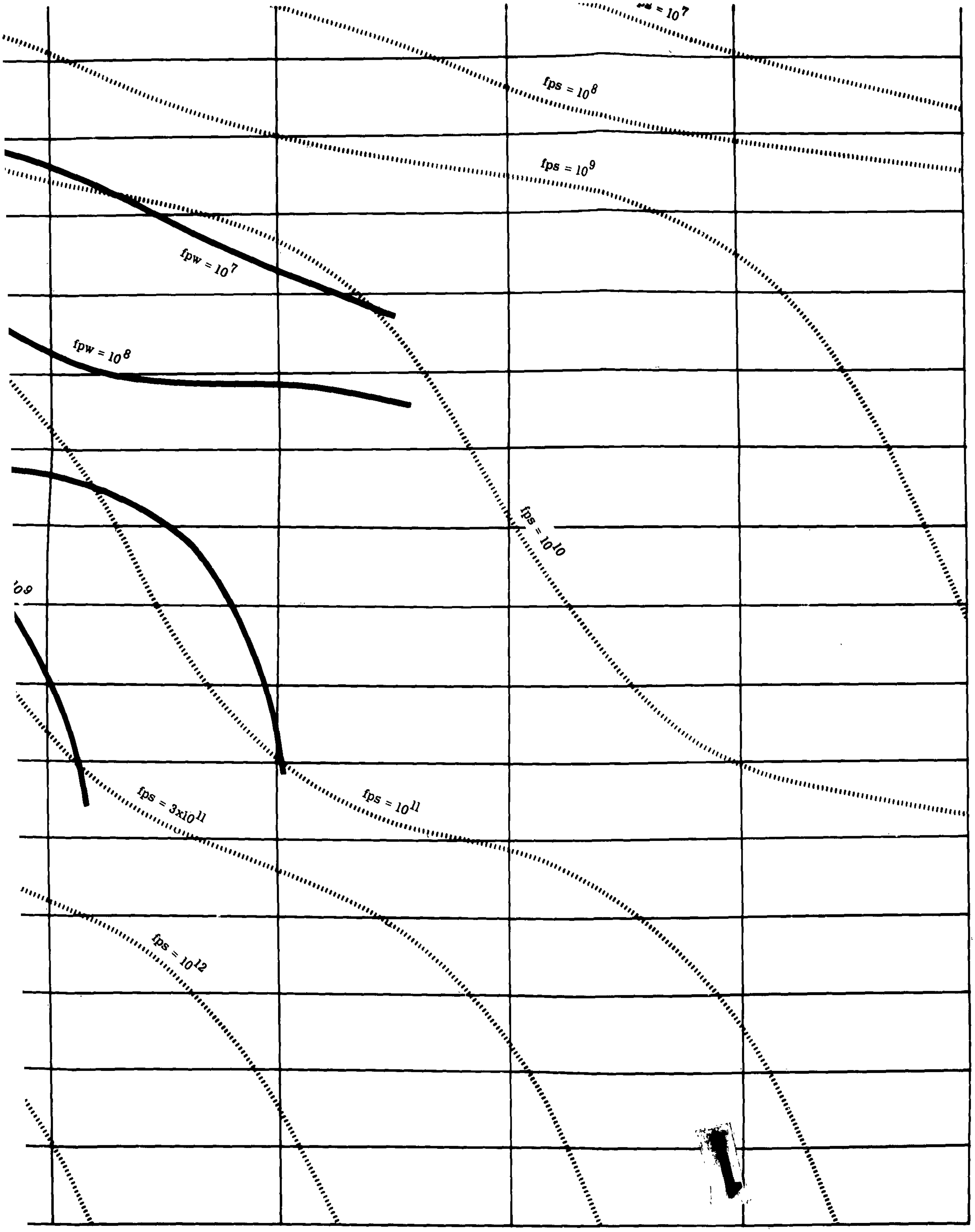
fps = 10^7
fps = 10^8
fps = 10^9
fpw = 10^7
fpw = 10^8
fps = 10^{10}
fps = $3x10^{11}$
fps = 10^{11}
fps = 10^{12}

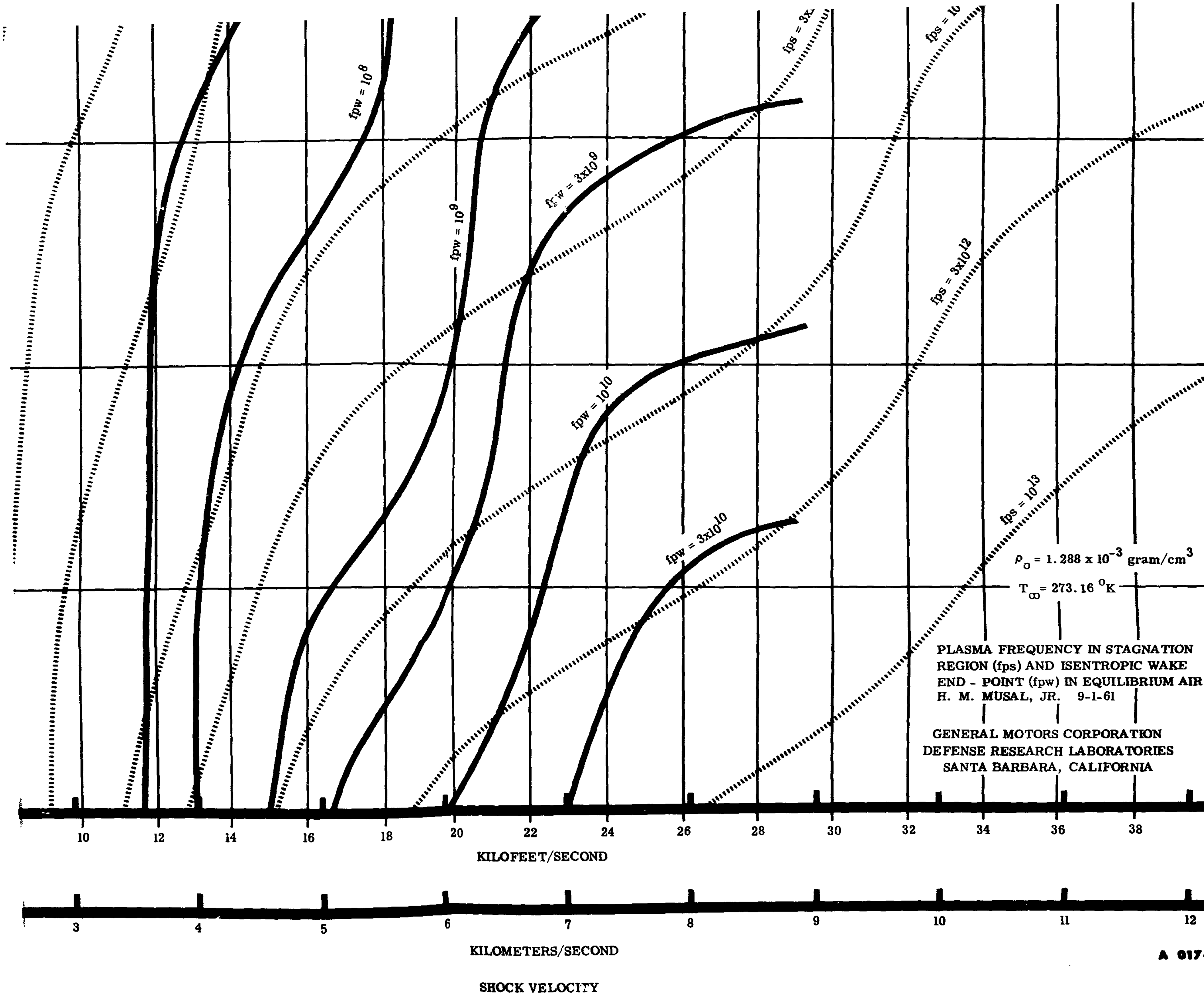

fpw = 10^8
fpw = 10^9
fpw = $3x10^9$
fpw = 10^{10}
fpw = $3x10^{10}$
fps = $3x10^{12}$
fps = 10^{13}
ρ_o = 1.288 x 10^{-3} gram/cm^3
T_∞ = 273.16 ^oK
PLASMA FREQUENCY IN STAGNATION
REGION (fps) AND ISENTROPIC WAKE
END - POINT (fpw) IN EQUILIBRIUM AIR
H. M. MUSAL, JR. 9-1-61
GENERAL MOTORS CORPORATION
DEFENSE RESEARCH LABORATORIES
SANTA BARBARA, CALIFORNIA
10
12
14
16
18
20
22
24
26
28
30
32
34
36
38
KILOFEET/SECOND
3
4
5
6
7
8
9
10
11
12
KILOMETERS/SECOND
SHOCK VELOCITY
A 0174

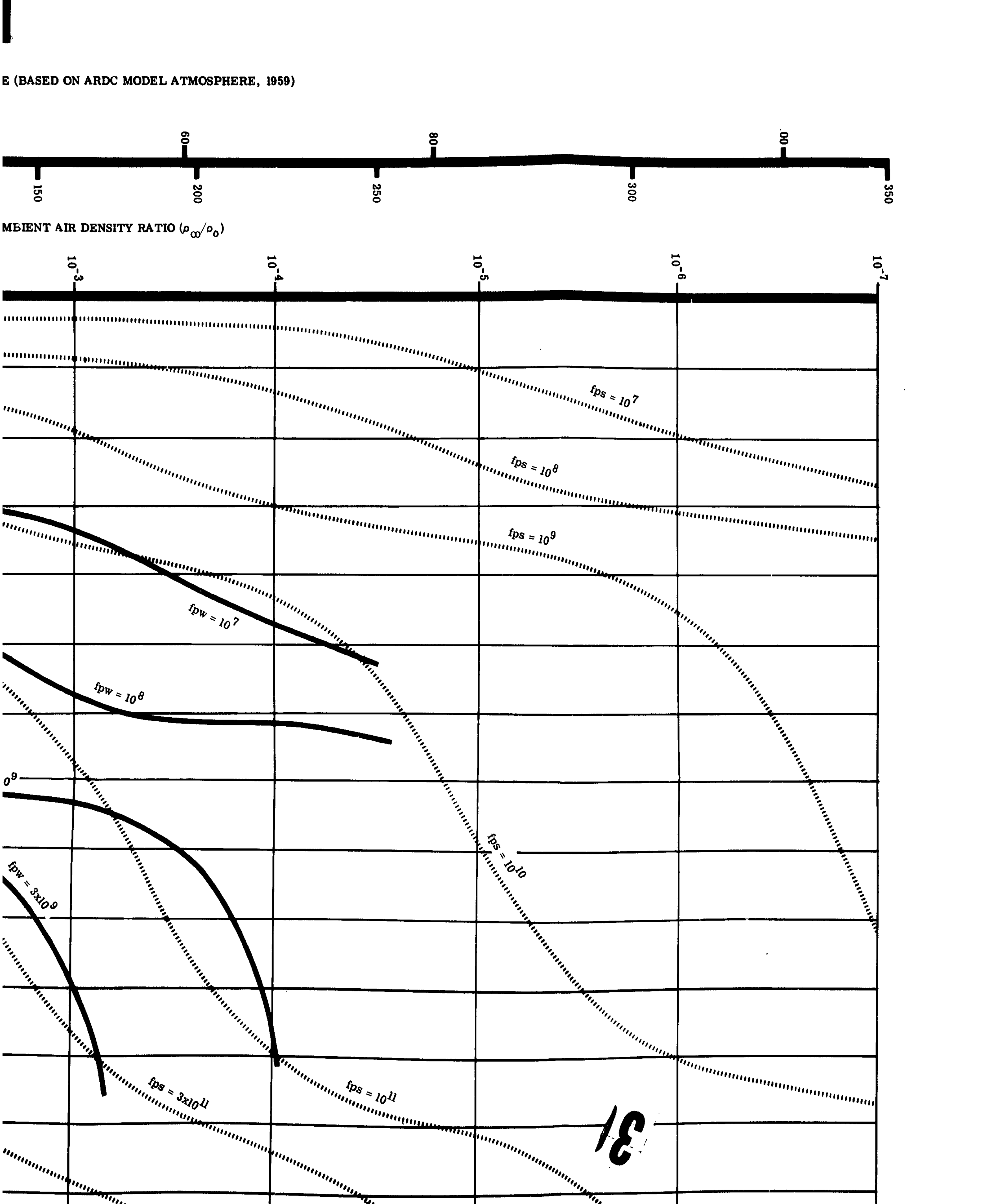
E (BASED ON ARDC MODEL ATMOSPHERE, 1959)
60
80
00
150
200
250
300
350
MBIENT AIR DENSITY RATIO (ρ_∞/ρ_0)
10^{-3}
10^{-4}
10^{-5}
10^{-6}
10^{-7}
fps = 10^7
fps = 10^8
fps = 10^9
fps = 10^{10}
fps = 10^{11}
fps = $3x10^{11}$
fpw = 10^7
fpw = 10^8
fpw = $3x10^9$
0^9
31

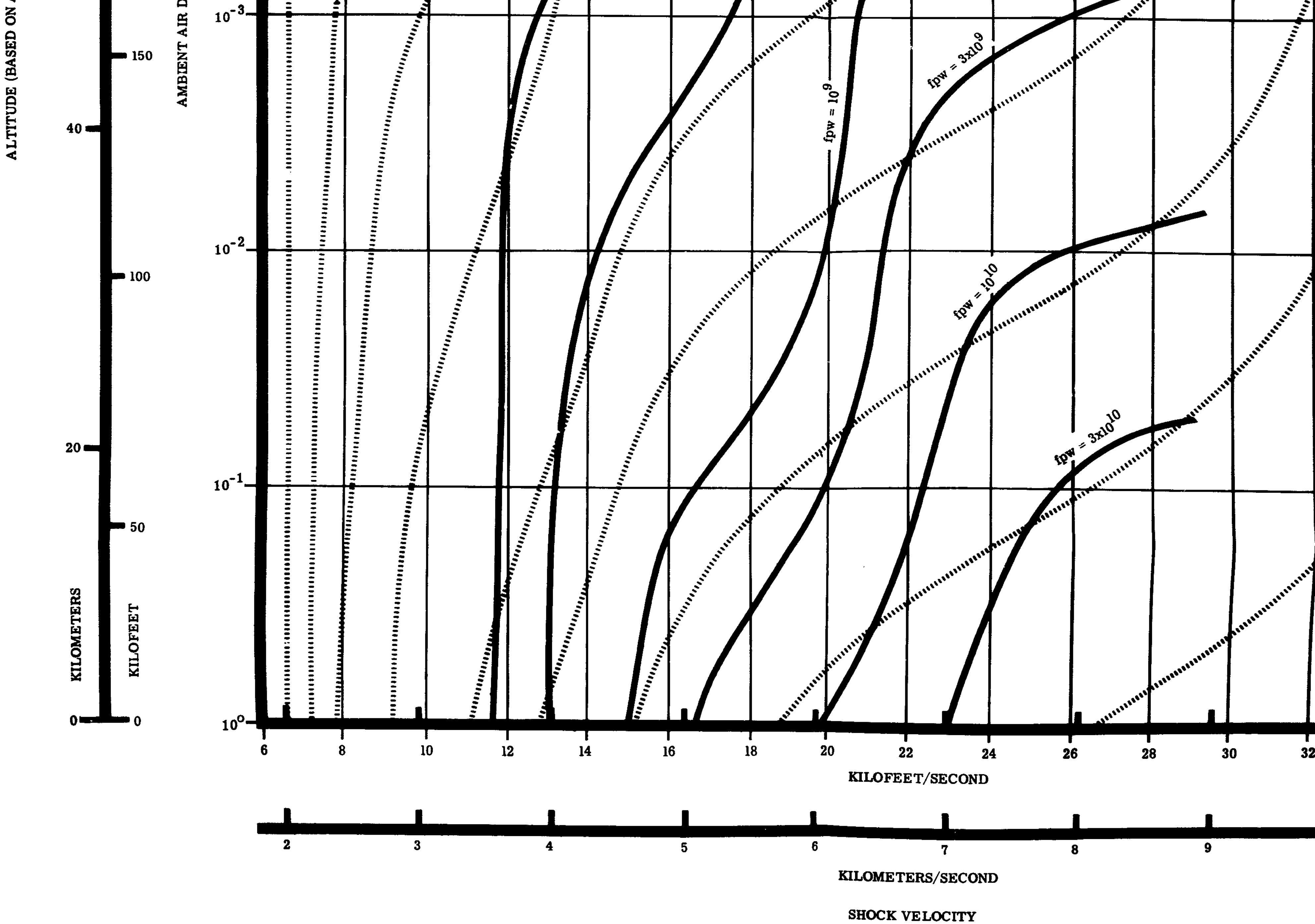

ALTITUDE (BASED ON
AMBIENT AIR D
KILOMETERS
KILOFEET
0
20
40
0
50
100
150
10^{-3}
10^{-2}
10^{-1}
10^{0}
fpw = 10^9
fpw = $3x10^9$
fpw = 10^{10}
fpw = $3x10^{10}$
6
8
10
12
14
16
18
20
22
24
26
28
30
32
KILOFEET/SECOND
2
3
4
5
6
7
8
9
KILOMETERS/SECOND
SHOCK VELOCITY

$\nu_c = 10^6$
$\nu_c = 3 \times 10^6$
$f_p = 10^7$
$f_p = 10^8$
$\nu_c = 10^7$
$f_p = 10^9$
$\nu_c = 3 \times 10^7$
$f_p = 3 \times 10^9$
$\nu_c = 10^8$

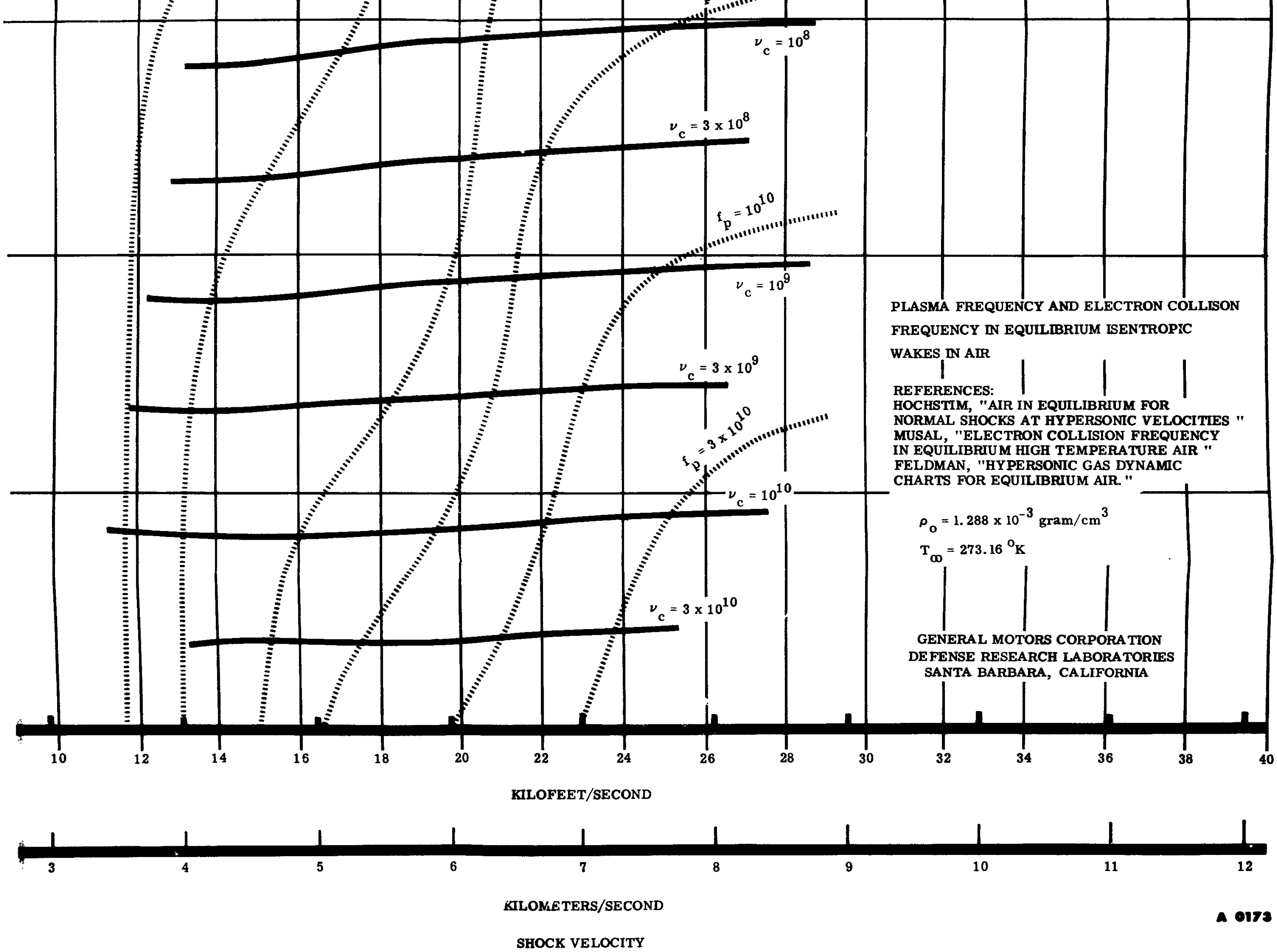

PLASMA FREQUENCY AND ELECTRON COLLISON FREQUENCY IN EQUILIBRIUM ISENTROPIC WAKES IN AIR
REFERENCES:
HOCHSTIM, "AIR IN EQUILIBRIUM FOR NORMAL SHOCKS AT HYPERSONIC VELOCITIES "
MUSAL, "ELECTRON COLLISION FREQUENCY IN EQUILIBRIUM HIGH TEMPERATURE AIR "
FELDMAN, "HYPERSONIC GAS DYNAMIC CHARTS FOR EQUILIBRIUM AIR. "
$\rho_o = 1.288 \times 10^{-3}$ gram/cm^3
$T_\infty = 273.16\ ^oK$
GENERAL MOTORS CORPORATION
DEFENSE RESEARCH LABORATORIES
SANTA BARBARA, CALIFORNIA
$\nu_c = 10^8$
$\nu_c = 3 \times 10^8$
$f_p = 10^{10}$
$\nu_c = 10^9$
$\nu_c = 3 \times 10^9$
$f_p = 3 \times 10^{10}$
$\nu_c = 10^{10}$
$\nu_c = 3 \times 10^{10}$
10
12
14
16
18
20
22
24
26
28
30
32
34
36
38
40
KILOFEET/SECOND
3
4
5
6
7
8
9
10
11
12
KILOMETERS/SECOND
SHOCK VELOCITY
A 0173

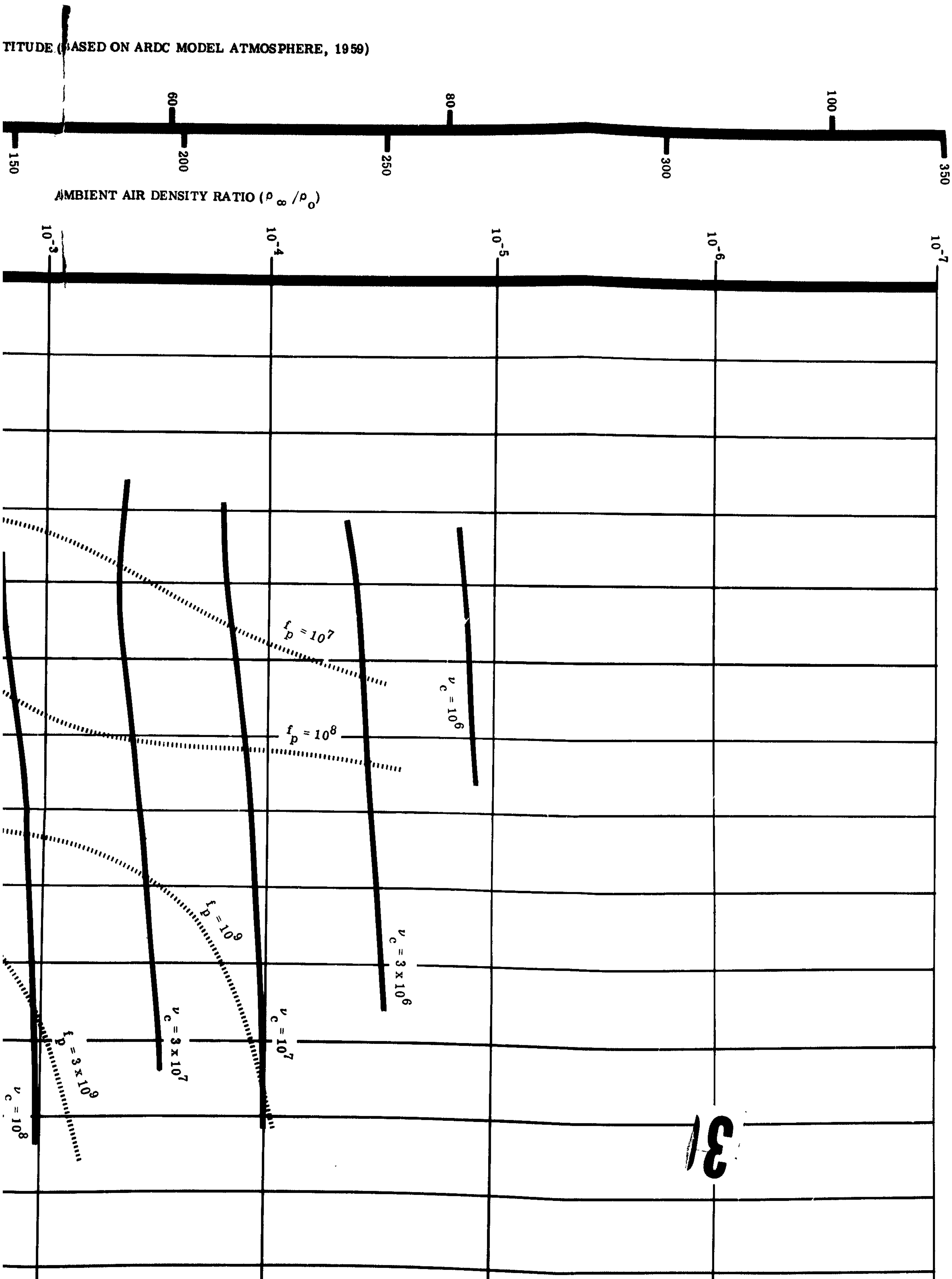

TITUDE (BASED ON ARDC MODEL ATMOSPHERE, 1959)
60
80
100
150
200
250
300
350
AMBIENT AIR DENSITY RATIO (ρ_∞/ρ_o)
10^{-3}
10^{-4}
10^{-5}
10^{-6}
10^{-7}
$f_p = 10^7$
$f_p = 10^8$
$f_p = 10^9$
$f_p = 3 \times 10^9$
$\nu_c = 10^6$
$\nu_c = 3 \times 10^6$
$\nu_c = 10^7$
$\nu_c = 3 \times 10^7$
$\nu_c = 10^8$

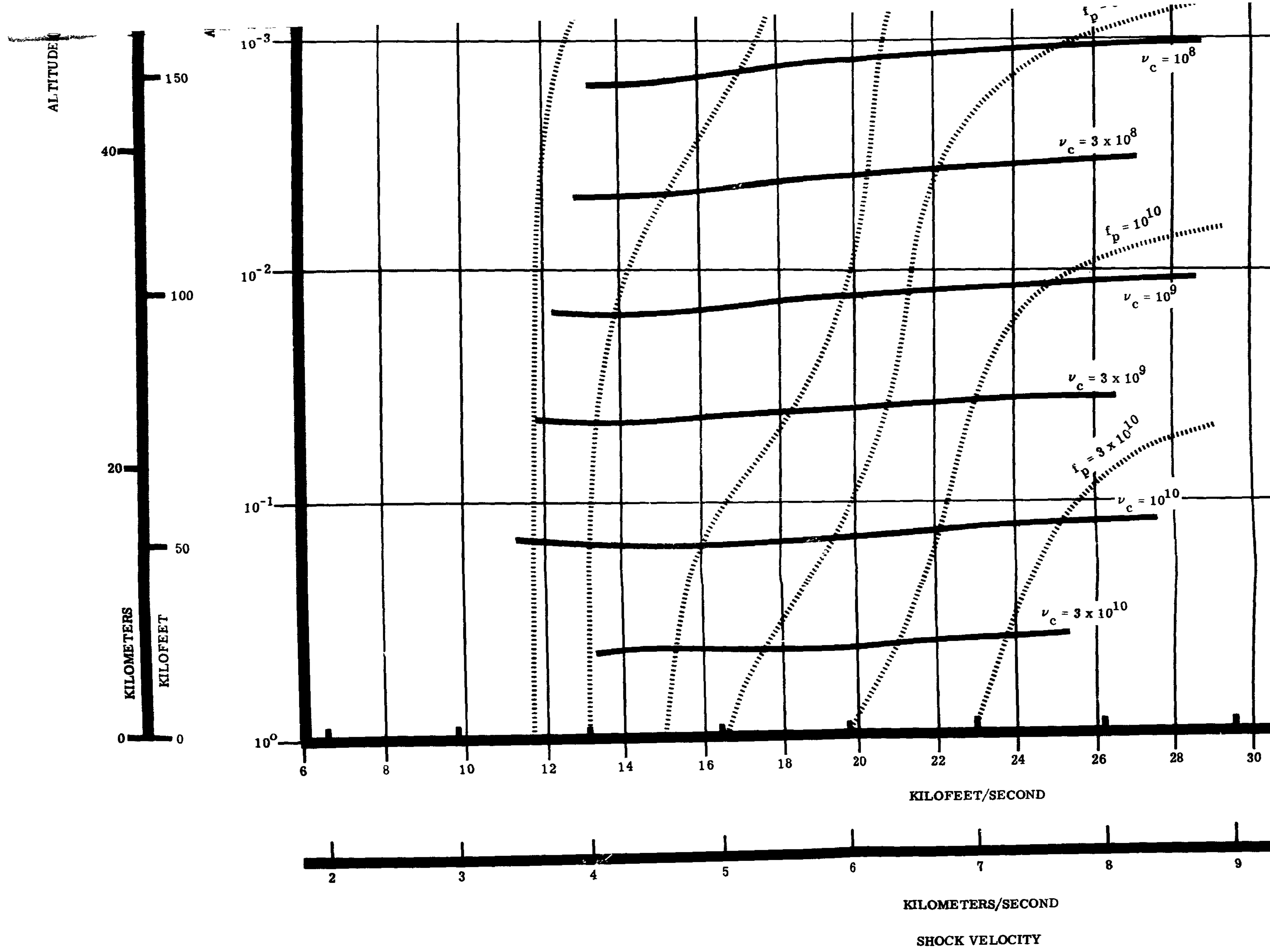

PLASMA
FREQUE
WAKES I

REFERE
HOCHSTI
NORMAI
MUSAL,
IN EQUI
FELDMA
CHARTS

ρ_o =
T_∞ =

GENE
DEFEN
SAN

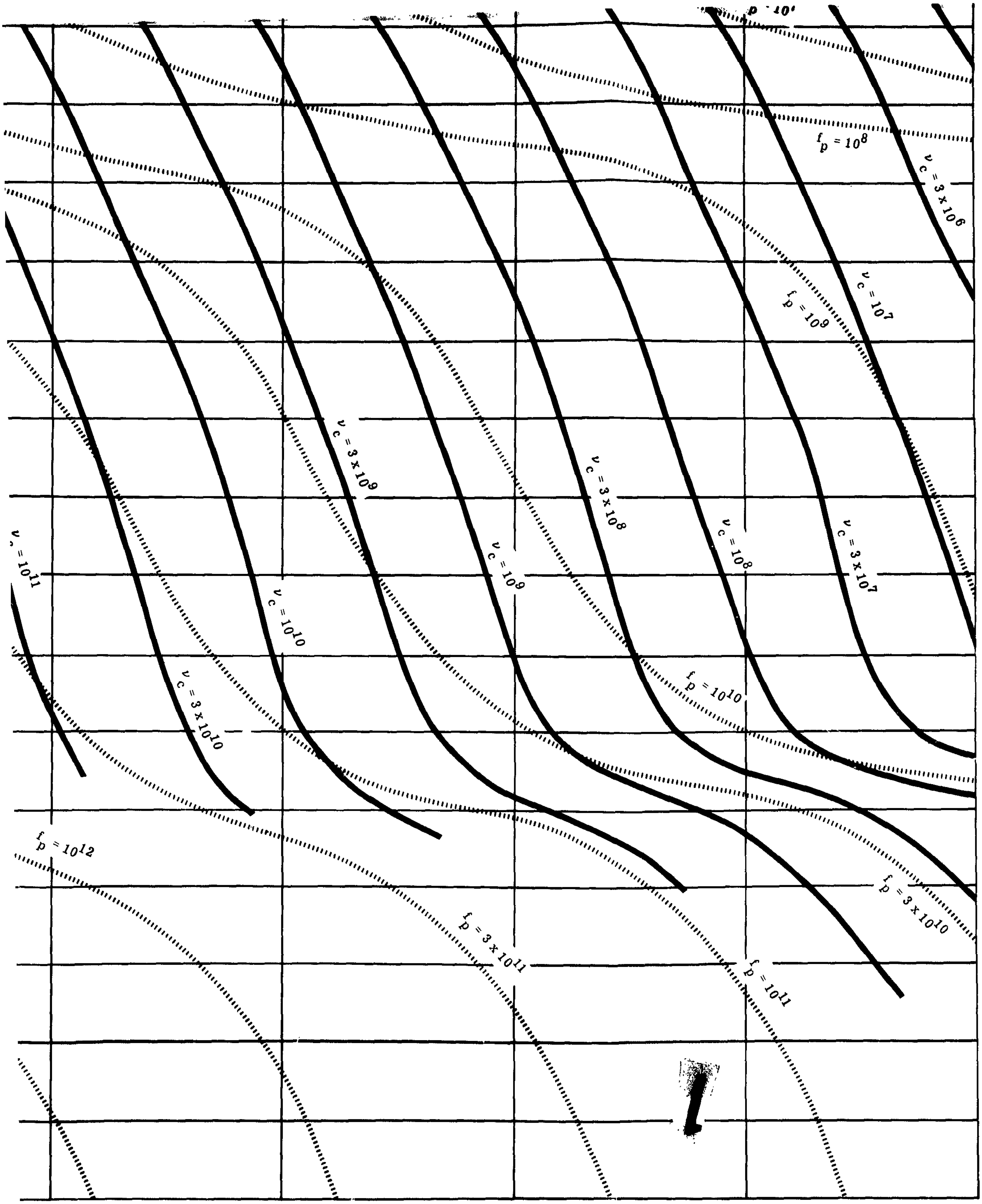

$f_p = 10^8$
$f_p = 10^9$
$f_p = 10^{10}$
$f_p = 3 \times 10^{10}$
$f_p = 10^{11}$
$f_p = 3 \times 10^{11}$
$f_p = 10^{12}$
$\nu_c = 3 \times 10^6$
$\nu_c = 10^7$
$\nu_c = 3 \times 10^7$
$\nu_c = 10^8$
$\nu_c = 3 \times 10^8$
$\nu_c = 10^9$
$\nu_c = 3 \times 10^9$
$\nu_c = 10^{10}$
$\nu_c = 3 \times 10^{10}$
$\nu_c = 10^{11}$

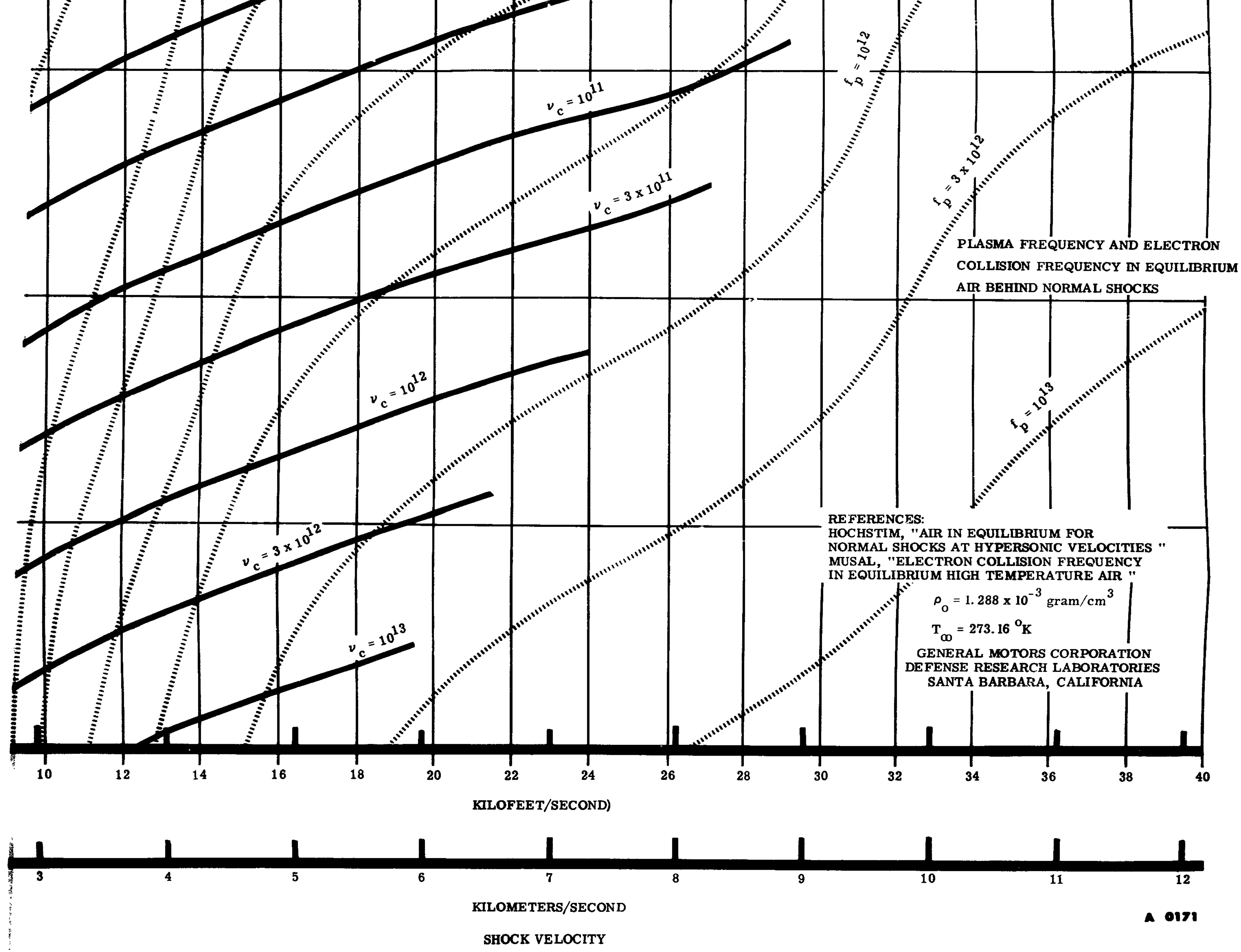

PLASMA FREQUENCY AND ELECTRON COLLISION FREQUENCY IN EQUILIBRIUM AIR BEHIND NORMAL SHOCKS
$\nu_c = 10^{11}$
$\nu_c = 3 \times 10^{11}$
$\nu_c = 10^{12}$
$\nu_c = 3 \times 10^{12}$
$\nu_c = 10^{13}$
$f_p = 10^{12}$
$f_p = 3 \times 10^{12}$
$f_p = 10^{13}$
REFERENCES:
HOCHSTIM, "AIR IN EQUILIBRIUM FOR NORMAL SHOCKS AT HYPERSONIC VELOCITIES "
MUSAL, "ELECTRON COLLISION FREQUENCY IN EQUILIBRIUM HIGH TEMPERATURE AIR "
$\rho_o = 1.288 \times 10^{-3}$ gram/cm^3
$T_\infty = 273.16$ °K
GENERAL MOTORS CORPORATION
DEFENSE RESEARCH LABORATORIES
SANTA BARBARA, CALIFORNIA
10 12 14 16 18 20 22 24 26 28 30 32 34 36 38 40
KILOFEET/SECOND)
3 4 5 6 7 8 9 10 11 12
KILOMETERS/SECOND
SHOCK VELOCITY
A 0171

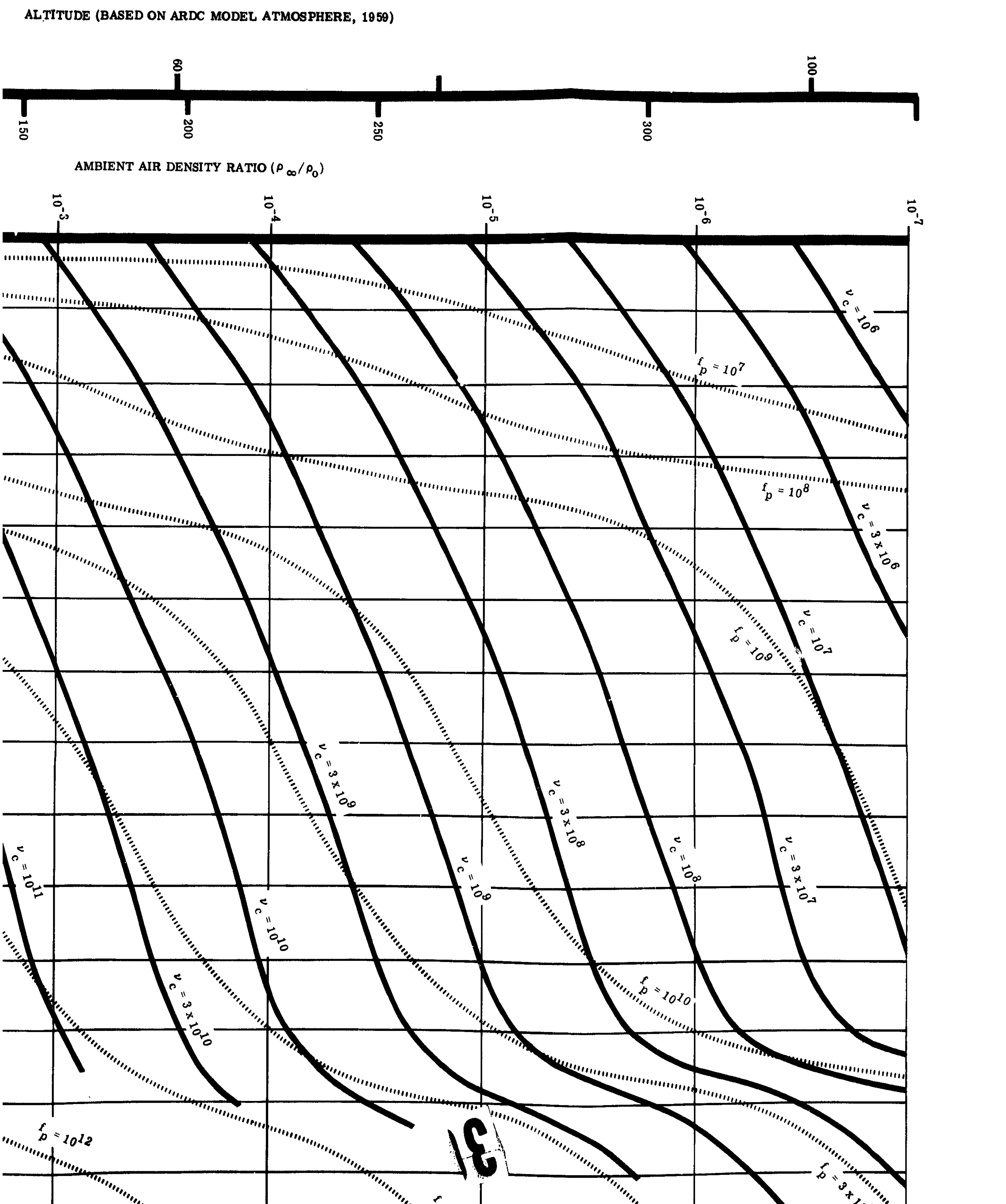

ALTITUDE (BASED ON ARDC MODEL ATMOSPHERE, 1959)
60
100
150
200
250
300
AMBIENT AIR DENSITY RATIO (ρ_∞/ρ_0)
10^{-3}
10^{-4}
10^{-5}
10^{-6}
10^{-7}
$\nu_c = 10^6$
$f_p = 10^7$
$f_p = 10^8$
$\nu_c = 3 \times 10^6$
$\nu_c = 10^7$
$f_p = 10^9$
$\nu_c = 3 \times 10^9$
$\nu_c = 3 \times 10^8$
$\nu_c = 10^8$
$\nu_c = 3 \times 10^7$
$\nu_c = 10^{11}$
$\nu_c = 10^9$
$\nu_c = 10^{10}$
$f_p = 10^{10}$
$\nu_c = 3 \times 10^{10}$
$f_p = 10^{12}$
31

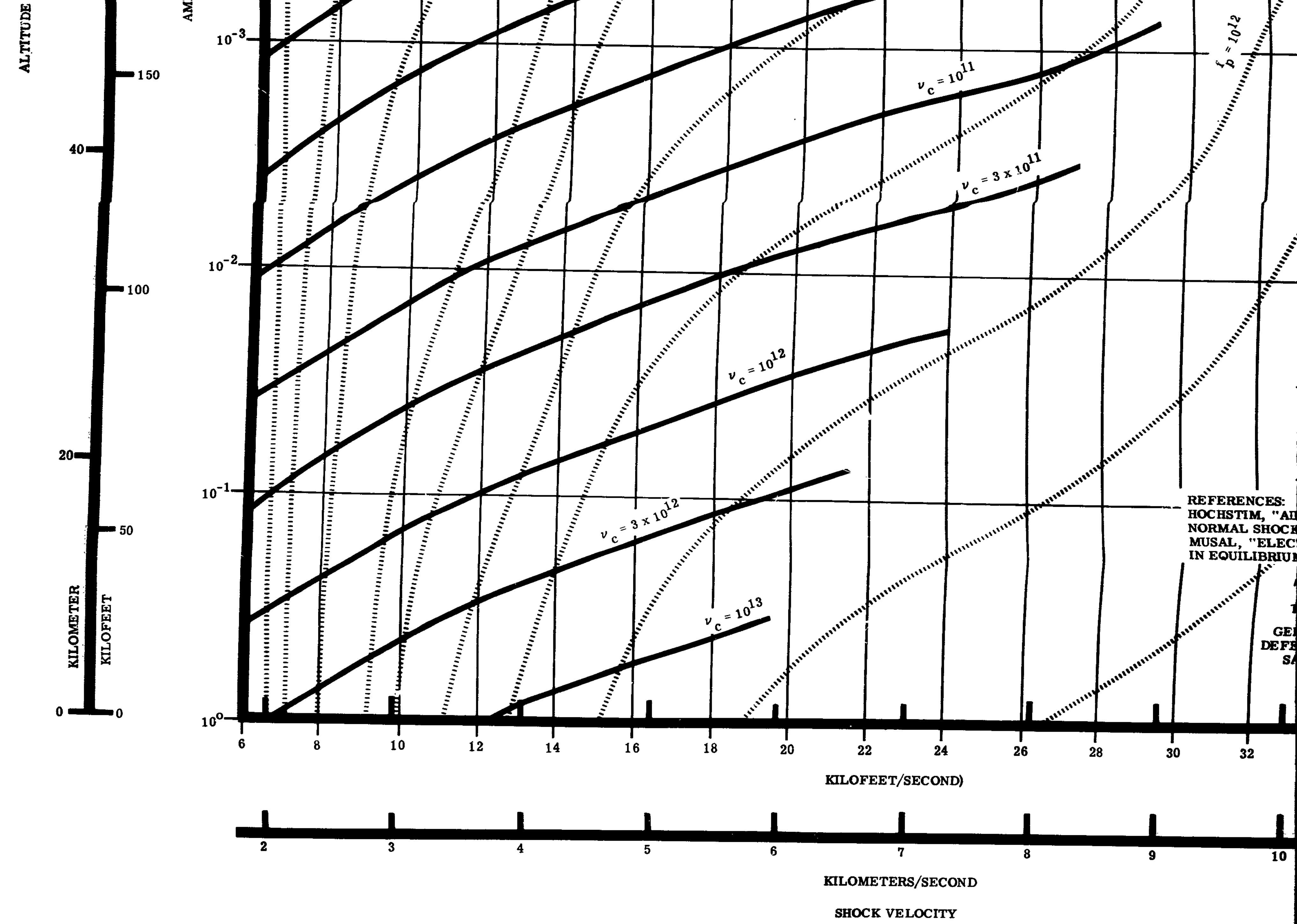

ALTITUDE
KILOMETER
KILOFEET
0
20
40
0
50
100
150
AM
10^{-3}
10^{-2}
10^{-1}
10^{0}
$\nu_c = 10^{11}$
$\nu_c = 3 \times 10^{11}$
$\nu_c = 10^{12}$
$\nu_c = 3 \times 10^{12}$
$\nu_c = 10^{13}$
$f_p = 10^{12}$
6
8
10
12
14
16
18
20
22
24
26
28
30
32
KILOFEET/SECOND)
2
3
4
5
6
7
8
9
10
KILOMETERS/SECOND
SHOCK VELOCITY
REFERENCES:
HOCHSTIM, "AI
NORMAL SHOCK
MUSAL, "ELEC
IN EQUILIBRIU